

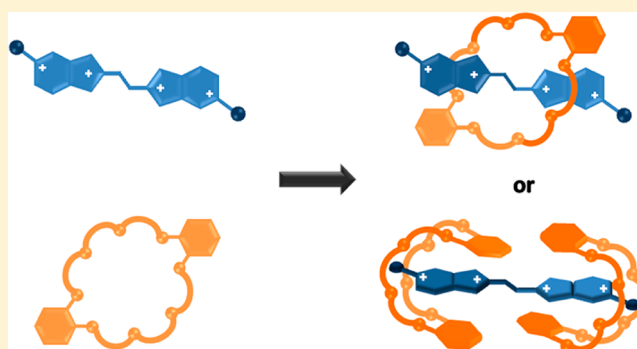
Complexation of Imidazopyridine-Based Cations with a 24-Crown-8 Ether Host: [2]Pseudorotaxane and Partially Threaded Structures

Surisadai I. Moreno-Olivares, Ruy Cervantes, and Jorge Tiburcio*

Departamento de Química, Centro de Investigación y de Estudios Avanzados (Cinvestav), Avenida IPN 2508, Zacatenco 07360, México D. F., México

S Supporting Information

ABSTRACT: A new series of linear molecules derived from 1,2-bis(imidazopyridin-2-yl)ethane can fully or partially penetrate the cavity of the dibenzo-24-crown-8 macrocycle to produce a new family of host–guest complexes. Protonation or alkylation of the nitrogen atoms on the pyridine rings led to an increase in the guest total positive charge up to 4+ and simultaneously generated two new recognition sites (pyridinium motifs) that are in competition with the 1,2-bis-(benzimidazole)ethane motif for the crown ether. The relative position of the pyridine ring and the chemical nature of the N-substituent determined the preferred motif and the host–guest complex geometry: (i) for linear guests with relatively bulky groups (i.e., a benzyl substituent), the 1,2-bis(benzimidazole)ethane motif is favored, leading to a fully threaded complex with a [2]pseudorotaxane geometry; (ii) for small substituents, such as –H and –CH₃ groups, regardless of the guest shape, the pyridinium motifs are preferred, leading to external partially threaded complexes in a 2:1 host to guest stoichiometry.



INTRODUCTION

The development of molecular devices based on interlocked molecules, such as rotaxanes and catenanes, requires specific control of the relative position of their components.¹ The most successful approach to the synthesis of this kind of supramolecular system relies on the use of a template.² Among templates, the cationic imidazolium motif has proved to be a versatile guest for various hosts such as those based on isophthalamide,³ cyclodextrin,⁴ cucurbituril,⁵ calixarene,⁶ pillararene,⁷ cyclophanes,⁸ and crown ethers.^{9,10}

Recently, Loeb and co-workers reported the synthesis of [2]rotaxane molecular shuttles based on a bis(benzimidazole) axle and a variety of macrocyclic crown ethers with a relatively short linear pathway along the axle. In these systems, the shuttling can be acid–base-controlled, and its rate depends on the nature of the macrocycle.¹⁰

In a previous work, we reported that protonated versions of different 1,2-bis(benzimidazol-2-yl)ethane derivatives form stable inclusion complexes with the dibenzo-24-crown-8 ether (DB24C8) macrocycle in a [2]pseudorotaxane geometry both in solution and in the solid state.^{9a} These pseudorotaxanes are held together by a series of non-covalent interactions, such as (+)N–H...O charge-assisted hydrogen bonding, ion–dipole, and π -stacking interactions. It was proved that an increase in the association constant could be achieved with the presence of electron-withdrawing groups on the axle, which favors electrostatic interactions between the components.

Now we propose a modification of the 1,2-bis(benzimidazol-2-yl)ethane derivatives by introducing pyridine rings fused to the imidazole moieties at two different positions, giving rise to a new family of 1,2-bis(imidazopyridin-2-yl)ethane compounds (Scheme 1). The inclusion of pyridine rings allows the incorporation of two extra positive charges by protonation or alkylation, enhancing the electron-poor character of the axle and, in principle, favoring the host–guest interaction with DB24C8. Depending on the relative position of the pyridine ring and the chemical nature of the N-substituent, we expect variations on the geometry of the host–guest complex. Herein we report the design, synthesis, and solution NMR and X-ray crystallographic studies of N-functionalized axles derived from 1,2-bis(imidazopyridine-2-yl)ethane cations and their host–guest chemistry with dibenzo-24-crown-8 ether.

RESULTS AND DISCUSSION

Imidazopyridine-Based Cationic Guests. The 1,2-bis-(imidazopyridin-2-yl)ethane compounds were prepared by a condensation reaction between succinic acid and the corresponding diaminopyridine (3,4-diaminopyridine for compound [2] and 2,3-diaminopyridine for compound [3]) under acidic conditions (Scheme 2A). The N-alkyl or N-benzyl derivatives [2·R₂]²⁺ and [3·R₂]²⁺ (R = Me, Bn, tBuBn) were obtained in good yields by direct alkylation of precursors [2] and [3] with an excess of the corresponding alkyl halide

Received: August 3, 2013

Published: October 1, 2013

well as HR-MS (ESI-TOF); compounds $[2\cdot\text{Bn}_2][\text{CF}_3\text{SO}_3]_2$ and $[3\cdot\text{Bn}_2]\text{Br}_2$ were also characterized by single-crystal X-ray diffraction.

All of the compounds displayed a single resonance for the ethylene bridge, indicative of an inversion center in the molecule; an ABC pattern for the aromatic protons of the pyridine rings was also observed, regardless of the substituent on the nitrogen atom. Additionally, the NMR spectra showed the resonances expected for the different R groups. The experimental high-resolution mass spectra (ESI-TOF) were consistent with the proposed formulas and the calculated isotopic patterns; in all cases the relative errors in the molecular weights were less than 3 ppm.

Crystals suitable for X-ray diffraction analysis of $[2\cdot\text{Bn}_2][\text{CF}_3\text{SO}_3]_2$ were obtained from an aqueous solution containing $[2\cdot\text{Bn}_2][\text{Br}]_2$ and sodium trifluoromethanesulfonate. The isolated crystals belong to the monoclinic space group $P2_1/c$. A crystallographic inversion center is located along the $-\text{CH}_2-\text{CH}_2-$ bond, rendering one-half of the cation, one water molecule, and one trifluoromethanesulfonate per asymmetric unit. The ethane bridge adopts an *anti* conformation that induces a linear shape on the cation, and the two benzyl groups are also in an *anti* arrangement. A hydrogen-bonding network is formed between water molecules ($\text{O}_w\cdots\text{O}_{\text{Trf}}$ 3.02 Å; $\text{O}_w-\text{H}_w\cdots\text{O}_{\text{Trf}}$ 163.6°), trifluoromethanesulfonate counterions [$\text{O}_{\text{Trf}}\cdots\text{N}(\text{H})$, 2.79 Å; $\text{O}_{\text{Trf}}\cdots\text{H}-\text{N}$, 168.2°], and the imidazolium rings ($\text{N}-\text{O}_w$ 3.02 Å; $\text{N}\cdots\text{H}_w-\text{O}_w$ 165.4°), stabilizing the crystal lattice. Figure 1 shows the molecular structure in the solid state for this compound.

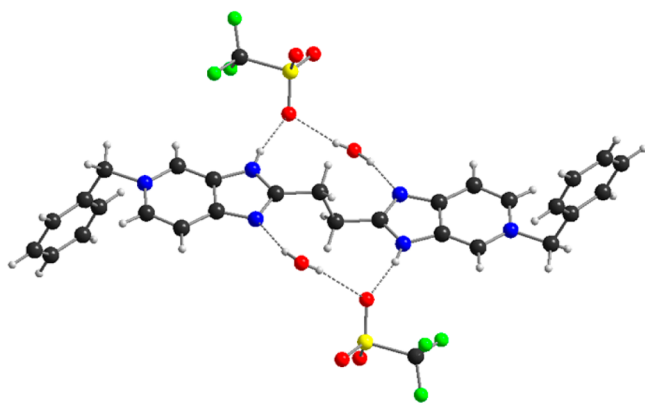


Figure 1. Ball-and-stick representation of the molecular structure of $[2\cdot\text{Bn}_2][\text{CF}_3\text{SO}_3]_2$ determined by single-crystal X-ray diffraction. N = blue, C = black, O = red, F = green, S = yellow, H = white.

Single crystals of $[3\cdot\text{Bn}_2]\text{Br}_2$ were also analyzed by X-ray diffraction. The isolated crystals belong to the monoclinic space group $P2_1/n$. A complete molecule, two bromide anions, and one chloroform molecule are contained in the asymmetric unit. In clear contrast to $[2\cdot\text{Bn}_2][\text{CF}_3\text{SO}_3]_2$, the ethane bridge in compound $[3\cdot\text{Bn}_2]\text{Br}_2$ adopts a *gauche* conformation with a torsion angle of 71° (Figure 2), resulting in a nonlinear arrangement of the molecular structure. Bromide anions act as bridges between two different imidazopyridine cations through $\text{Br}\cdots\text{H}-\text{N}$ hydrogen bonding, with $\text{Br}\cdots\text{N}$ distances varying from 3.1 to 3.6 Å and $\text{N}-\text{H}\cdots\text{Br}$ angles between 171 and 172°.

In order to switch on the molecular recognition process and generate host–guest complexes, all of the imidazopyridine derivatives were protonated in acetonitrile with the corresponding equivalents of trifluoromethanesulfonic acid to yield the tetracationic axes $[2\cdot\text{H}_4]^{4+}$, $[3\cdot\text{H}_4]^{4+}$, $[2\cdot\text{R}_2\text{H}_2]^{4+}$, and $[3\cdot\text{R}_2\text{H}_2]^{4+}$ (R = Me, Bn, *t*BuBn); then 1 equiv of DB24C8 was added to each one of the protonated compounds. The host–guest complexes

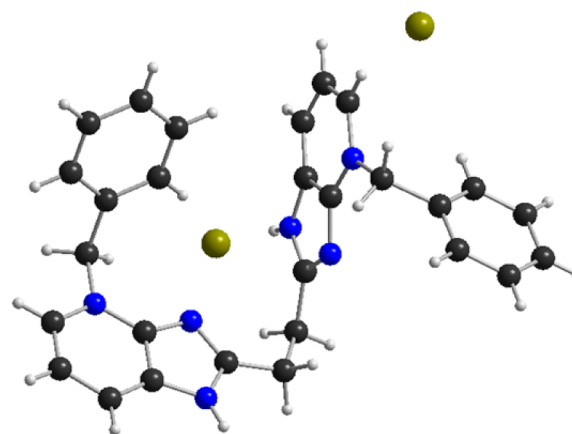


Figure 2. Ball-and-stick representation of the molecular structure of $[3\cdot\text{Bn}_2]\text{Br}_2$ determined by single-crystal X-ray diffraction. N = blue, C = black, Br = green, H = white. The solvent molecule has been omitted for clarity.

were investigated in solution by ^1H NMR and ESI-MS analyses, and the complex between $[2\cdot\text{Bn}_2\text{H}_2]^{4+}$ and DB24C8 was also studied in the solid state by single-crystal X-ray diffraction. Regarding the geometry of the complexes, two different arrangements were observed: (i) fully threaded (i.e., $[2]$ pseudorotaxane) and (ii) partially threaded.

[2]Pseudorotaxane Geometry. This behavior was observed only for cation $[2\cdot\text{Bn}_2\text{H}_2]^{4+}$, which was prepared in situ by the addition of 2 equiv of trifluoromethanesulfonic acid to a 5×10^{-3} M solution of compound $[2\cdot\text{Bn}_2][\text{CF}_3\text{SO}_3]_2$ in CD_3CN . Upon addition of 1 equiv of DB24C8, the ^1H NMR spectrum (Figure 3) showed two different sets of signals, suggesting the formation of a host–guest complex in a slow association/dissociation process with the free components on the NMR time scale. All of the pyridinium ring signals for the complex appeared at lower frequencies with respect to the free axle (H_a , $\Delta\delta = -0.26$ ppm; H_b , $\Delta\delta = -0.07$ ppm; H_c , $\Delta\delta = -0.22$ ppm), with the most prominent effect observed for H_a and H_c as a consequence of the proximity of the electron-rich DB24C8 catechol rings. In sharp contrast, a displacement to higher frequency ($\Delta\delta = +0.27$ ppm) was observed for the ethylene bridge protons (H_d), which suggests $\text{C}-\text{H}\cdots\text{O}$ hydrogen bonding with crown ether oxygen atoms. These observations are indicative of a host–guest complex in a $[2]$ pseudorotaxane arrangement, in agreement with analogous reported systems.¹¹ According to the integral values of the associated complex signals, the stoichiometry was established as 1:1. The association constant, K_a , was determined to be $(1.3 \pm 0.1) \times 10^2 \text{ M}^{-1}$ by three independent measurements following the single-point method. Interestingly, this value is lower than the one obtained for the dicationic $[1\cdot\text{H}_2]^{2+}$ analogue with the same crown ether under identical conditions. This can be rationalized by an increase in the desolvation energy in passing from the dicationic guest $[1\cdot\text{H}_2]^{2+}$ to the tetracationic guest $[2\cdot\text{Bn}_2\text{H}_2]^{4+}$, which would compensate for or even surpass any stabilization energy gained by the addition of two extra positive charges on the $[2]$ pseudorotaxane complex.

The complex was also studied by electrospray ionization mass spectrometry. The mass spectrum showed a peak corresponding to $[2\cdot\text{Bn}_2 + \text{DB24C8} + \text{CF}_3\text{SO}_3]^+$ (calcd, m/z 1043.3831; found, m/z 1043.3821; error = 0.4 ppm) which is indicative of the association between the host and the guest in the gas phase.

The threaded geometry of the $[2]$ pseudorotaxane was confirmed by X-ray diffraction analysis (Figure 4). Single crystals

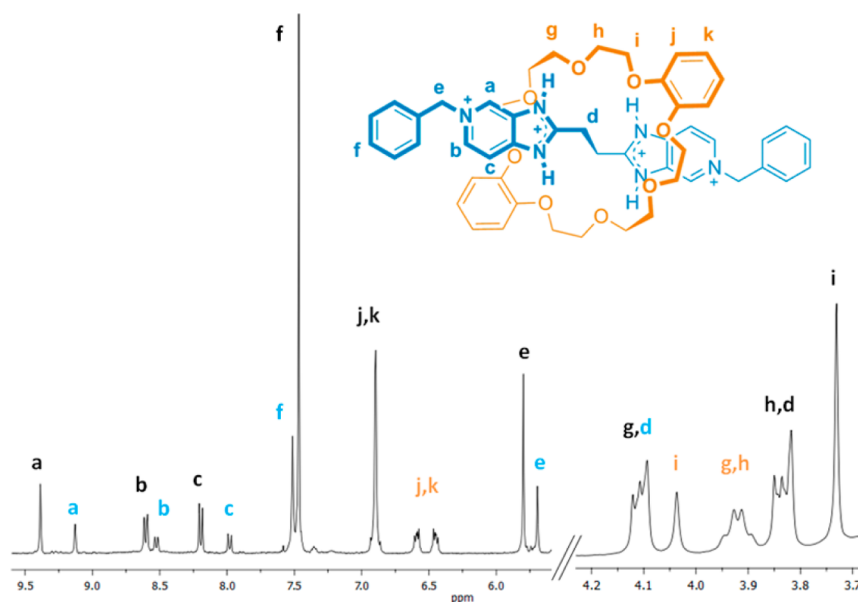


Figure 3. ^1H NMR spectrum (300 MHz, CD_3CN) of an equimolar solution (5×10^{-3} M) of $[\mathbf{2}\text{-Bn}_2\text{H}_2][\text{CF}_3\text{SO}_3]_4$ and DB24C8 . Orange and blue labels = $[\mathbf{2}]$ pseudorotaxane $[\mathbf{2}\text{-Bn}_2\text{H}_2\text{CDB24C8}]^{4+}$; black labels = uncomplexed host DB24C8 and guest $[\mathbf{2}\text{-Bn}_2\text{H}_2]^{4+}$.

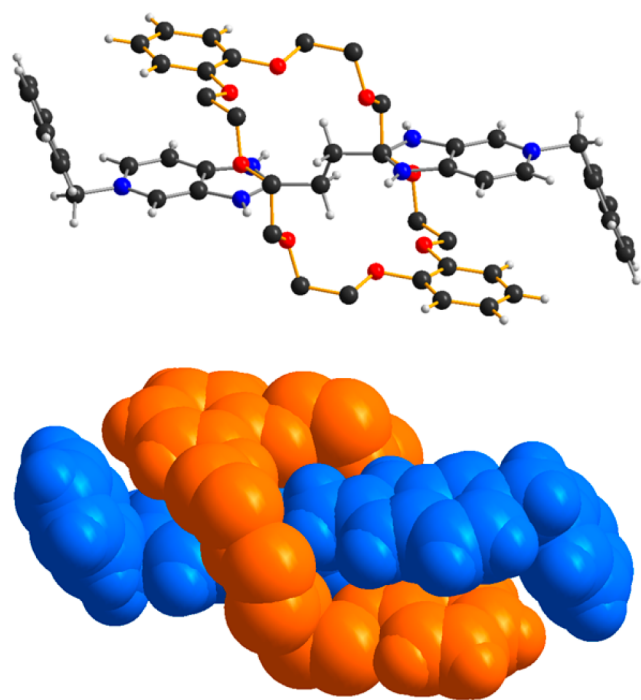


Figure 4. Ball-and-stick (top; N = blue, C = black, O = red, H = white) and space-filling (bottom; axle = blue, wheel = orange) representations of the $[\mathbf{2}]$ pseudorotaxane geometry of $[\mathbf{2}\text{-Bn}_2\text{H}_2\text{CDB24C8}]^{4+}$ determined by single-crystal X-ray diffraction. Counterions have been omitted for clarity.

were obtained by slow evaporation of an acetonitrile solution containing equimolar amounts of $[\mathbf{2}\text{-Bn}_2\text{H}_2][\text{CF}_3\text{SO}_3]_4$ and DB24C8 . The isolated crystals belong to the monoclinic space group $P2_1/n$; the $[\mathbf{2}]$ pseudorotaxane lies in a crystallographic inversion center, giving rise to only one-half of a host molecule and one-half of a guest molecule plus two trifluoromethanesulfonate counterions per asymmetric unit. The solid-state structure proves the completely interpenetrated conformation as well as the 1:1 stoichiometry. The ethylene moiety is located at the center of the crown ether cavity, and this arrangement is stabilized by the

formation of four weak hydrogen bonds ($\text{C}\cdots\text{O}$, 3.54 Å av; $\text{C}-\text{H}\cdots\text{O}$, 149° av). In addition, one of the $\text{N}-\text{H}$ groups from each imidazolium ring interacts with an oxygen atom of the crown ether, forming two strong hydrogen bonds ($\text{N}\cdots\text{O}$, 2.79 Å; $\text{N}-\text{H}\cdots\text{O}$, 154.2°). As clear evidence of an electrostatic ion–dipole interaction between the $[\mathbf{2}]$ pseudorotaxane components, one of the basic catechol oxygen atoms on DB24C8 is located over the center of the positively charged imidazolium ring at 3.2 Å. In addition, a distance of 3.5 Å between the planes formed by the catechol and pyridinium rings indicates some degree of $\pi-\pi$ interaction.

As expected, when the N -substituent is larger than the cavity of DB24C8 , such as a $t\text{BuBn}$ group, steric effects prevent the formation of an interpenetrated structure.¹² Therefore, ^1H NMR experiments showed no $[\mathbf{2}]$ pseudorotaxane formation or any other association mode between DB24C8 and $[\mathbf{2}\text{-(}t\text{BuBn)}_2\text{H}_2][\text{CF}_3\text{SO}_3]_4$ or $[\mathbf{3}\text{-(}t\text{BuBn)}_2\text{H}_2][\text{CF}_3\text{SO}_3]_4$ as the guest, discarding any kind of interaction between the imidazolium fragment and the crown ether.

Partially Threaded Geometry. The ^1H NMR spectra of equimolar solutions (2×10^{-3} M) of $[\mathbf{2}\text{-H}_4]^{4+}$ or $[\mathbf{2}\text{-Me}_2\text{H}_2]^{4+}$ and the macrocycle DB24C8 in CD_3CN showed only a single set of resonances with different chemical shifts relative to the parent compounds, suggesting the formation of a supramolecular complex. The fast exchange dynamics of the association/dissociation process on the NMR time scale is in clear contrast with the slow exchange process previously observed for the complex formed by the similar-sized analogue $[\mathbf{1}\text{-H}_2]^{2+}$ (see Scheme 1) and the same crown ether host. This last complex was established to self-assemble in a $[\mathbf{2}]$ pseudorotaxane geometry in solution and in the solid state.^{9a}

Further evidence of complexation between the crown ether and guests was obtained in the gas phase by high-resolution mass spectrometry (ESI-TOF). The mass spectra showed peaks corresponding to $[\mathbf{2}\text{-Me}_2 + \text{DB24C8} + \text{CF}_3\text{SO}_3]^+$ (calcd, m/z 891.3205; found, m/z 891.3230; error = 2.8 ppm) and $[\mathbf{2}\text{-H} + \text{DB24C8}]^+$ (calcd, m/z 713.3293; found, m/z 713.3303; error = 1.3 ppm).

To gain a better understanding of the stoichiometry and geometry of the host–guest complexes formed by $[\mathbf{2}\text{-H}_4]^{4+}$ and $[\mathbf{2}\text{-Me}_2\text{H}_2]^{4+}$ with DB24C8 , we carried out systematic ^1H

NMR experiments by following continuous variation and titration methods. The Job plots obtained for the systems DB24C8/[2·H₄]⁴⁺ and DB24C8/[2·Me₂H₂]⁴⁺ (Figure S1 in the Supporting Information) show maxima at a 0.66:0.33 molar ratio, indicating a 2:1 stoichiometry for both complexes in solution (i.e., two crown ethers per guest molecule). In the titration experiments, when saturation with DB24C8 was reached, the observed guest aromatic signals were shifted toward lower frequencies: [2·H₄]⁴⁺ (ppm) H_a Δδ = −0.21, H_b Δδ = −0.33, H_c Δδ = −0.17; [2·Me₂H₂]⁴⁺ (ppm): H_a Δδ = −0.21, H_b Δδ = −0.12, H_c Δδ = −0.37 (Figure 5 and Figure S2

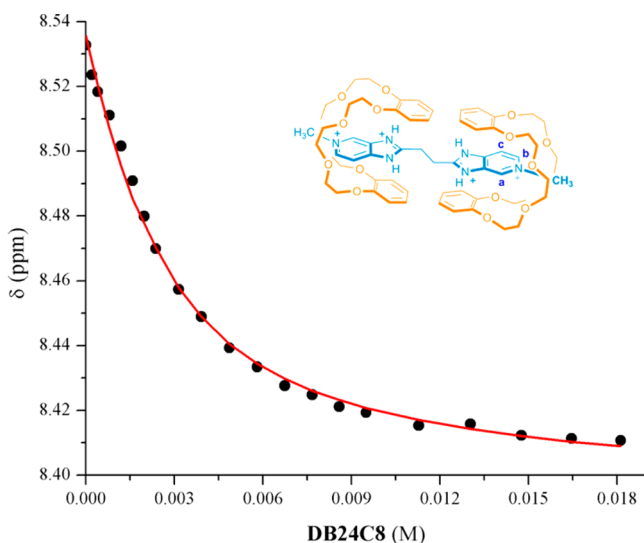


Figure 5. Chemical shift variation of proton H_b on the guest [2·Me₂H₂]⁴⁺ (2 mM) throughout the ¹H NMR titration with DB24C8 (0.1 M) in a CD₃CN solution. The inset shows the proposed structure of the complex.

in the Supporting Information).¹³ This behavior is characteristic of π -stacking interactions, probably between the electron-rich catechol rings on the crown ether and the electron-poor pyridinium rings on the guest. Additionally, the ethylene resonance signals for [2·H₄]⁴⁺ and [2·Me₂H₂]⁴⁺ were only slightly shifted toward lower frequencies ([2·H₄]⁴⁺, Δδ = −0.16 ppm; [2·Me₂H₂]⁴⁺, Δδ = −0.09 ppm), excluding the existence of any hydrogen bonding with the oxygen atoms on the crown ether. This observation is consistent with a nonthreaded geometry, in clear contrast to the one observed for guests [1·H₂]²⁺ and [2·Bn₂H₂]⁴⁺ with the same crown ether.

Furthermore, a NOESY experiment for an equimolar mixture of [2·Me₂H₂]⁴⁺ and DB24C8 (Figure S3 in the Supporting Information) revealed through-space coupling between the methyl protons on the cationic guest and the α and γ methylene protons on the crown ether host, suggesting spatial proximity of the guest methyl group and the crown ether cavity.

On the basis of these results, namely, (i) the fast-exchange host–guest association/dissociation process on the NMR time scale, (ii) the 2:1 host to guest stoichiometry, (iii) the guest chemical shift changes in the presence of the crown ether, and (iv) the NOESY cross-peaks between the methyl group on the cation and the hydrogen atoms on the crown ether cavity, we propose external complexation of two crown ether molecules to the guests [2·H₄]⁴⁺ and [2·Me₂H₂]⁴⁺ in a partially threaded geometry (Figure 5 inset), similar to analogous supramolecular complexes involving pyridinium guests,¹⁴ with π -stacking and ion–dipole interactions as the main contributions to the complex stability.

Table 1. Association Constants and Derived Free Energies of Association (ΔG°) of Guests [2·Bn₂H₂]⁴⁺, [2·H₄]⁴⁺, [2·Me₂H₂]⁴⁺, and [3·H₄]⁴⁺ with Host DB24C8

complex	association constant(s) (M ⁻¹) ^a	ΔG° (kJ mol ⁻¹) ^b
[2·Bn ₂ H ₂ ·CDB24C8] ⁴⁺	$K_a = (1.3 \pm 0.1) \times 10^2$	-12.1 ± 0.1
[2·H ₄ ·CDB24C8] ⁴⁺	$K_{a1} = (7.0 \pm 0.2) \times 10^2$ $K_{a2} = (8.8 \pm 0.3) \times 10^2$	-16.2 ± 0.4 -16.8 ± 0.6
[2·Me ₂ H ₂ ·CDB24C8] ⁴⁺	$K_{a1} = (6.5 \pm 0.3) \times 10^2$ $K_{a2} = (10.3 \pm 0.3) \times 10^2$	-16.0 ± 0.7 -17.2 ± 0.5
[3·H ₄ ·CDB24C8] ⁴⁺	$K_{a1} = (5.3 \pm 0.5) \times 10^2$ $K_{a2} = (12.0 \pm 0.8) \times 10^2$	-15.5 ± 1.4 -17.6 ± 1.2

^aDeterminations were made by ¹H NMR analysis in CD₃CN at 298 K. For the 1:1 complex [2·Bn₂H₂·CDB24C8]⁴⁺, the single-point method was used with a concentration of 5×10^{-3} M. For the other complexes, titration analyses were performed by least-squares fitting to a 2:1 host to guest model using a concentration of 2×10^{-3} M. ^b $\Delta G^\circ = -nRT \ln K_a$.

Association constants were derived from the experimental titration data (Table 1). The data were fitted to a 2:1 host to guest stoichiometry model using the least-squares method, affording two different K_a values. In all cases, the second association constant is slightly larger than the first, implying a reorganization of the guest upon complexation with the first crown ether molecule to render a more stable 2:1 host–guest complex. According to the measured association constants for tetracationic derivatives of compound [2], the pyridinium site is more favored with small substituents (R = H or CH₃), and only when this site is structurally hindered (as in the case of R = Bn) does the bis(benzimidazolium)ethane site become involved in complexation, resulting in a fully threaded geometry. Therefore, although our initial purpose was to promote [2]pseudorotaxane formation by the addition of two extra pyridinium rings in the guest, the result was instead a competition between two different recognition sites: pyridinium versus bis(benzimidazolium)ethane.

It is worth noticing that no complexation with DB24C8 was observed for guest [2·Me₂]²⁺, which indicates that the presence of the imidazolium ring in addition to the pyridinium motif is a requirement for complexation with the crown ether, although it is not directly involved in the interaction with the macrocycle. This can be rationalized by the strong electron-donating effect of the imidazole nitrogen atoms on the pyridinium ring, switching off the recognition site.

Effect of the Guest Shape on the Complexation.

Furthermore, when similar NMR experiments were made with compounds [3·Me₂H₂][CF₃SO₃]₄ and [3·Bn₂H₂][CF₃SO₃]₄ no evidence of association with DB24C8 was observed. The ¹H NMR spectra in CD₃CN showed only the corresponding signals for the nonassociated species. We hypothesize that the guest shape is responsible for the lack of association. The relative alkylation position between isomeric guests [2·R₂H₂]⁴⁺ and [3·R₂H₂]⁴⁺ (R = Bn, CH₃) modifies their shapes, controlling the complexation with DB24C8. On the other hand, cation [3·H₄]⁴⁺ displayed behavior similar to that of guest [2·H₄]⁴⁺ with DB24C8, as a partially threaded co-conformation appeared to be adopted around each pyridinium site (Table 1).

SUMMARY

A chemical modification of 1,2-bis(benzimidazol-2-yl)ethane cations led to a new family of tetracationic guests. These new guests possess

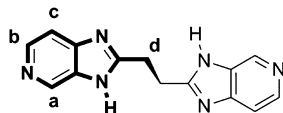
two pyridinium sites in addition to the bis(benzimidazolium)-ethane motif. On the basis of the guest shape and pyridinium substituent size, three different behaviors with **DB24C8** were observed: (i) for a linear guest with a benzyl substituent, a fully threaded complex with a [2]pseudorotaxane geometry involving the bis(benzimidazolium)ethane motif was formed; (ii) with hydrogen as the substituent regardless of the guest shape and with methyl as the substituent for the linear guest, external partially threaded complexes with a crown ether near each of the pyridinium sites were formed, with a host to guest stoichiometry of 2:1; and (iii) for nonlinear guests with bulkier substituents, no complexes were obtained.

EXPERIMENTAL SECTION

Materials and General Procedures. Dibenzo-24-crown-8, 2,3-diaminopyridine, 3,4-diaminopyridine, succinic acid, iodomethane, benzyl bromide, 4-*tert*-butylbenzyl bromide, sodium trifluoromethanesulfonate, trifluoromethanesulfonic acid, and polyphosphoric acid were commercially available and used as received. All solvents were of reagent grade and were dried and distilled prior to use. ^1H NMR spectra were recorded at 270, 300, or 400 MHz at 25 °C. ^1H - ^1H NMR COSY experiments were performed to confirm proton assignments. The following abbreviations are used for the multiplicities: s = singlet, d = doublet, dd = doublet of doublets, m = multiplet. ^{13}C NMR spectra were recorded at 68, 75, or 100 MHz at 25 °C. Chemical shifts are reported in parts per million relative to tetramethylsilane. High-resolution mass spectra were obtained on an electrospray ionization time-of-flight mass spectrometer. X-ray diffraction data were recorded with a CCD-detector-based diffractometer.

Synthesis of Neutral Compounds [2] and [3] and their corresponding cationic salts [2·H₄][CF₃SO₃]₄ and [3·H₄][CF₃SO₃]₄. Neutral compounds [2] and [3] were synthesized as follows. Succinic acid (0.236 g, 2.0 mmol) and the corresponding diaminopyridine (0.523 mg, 4.8 mmol) were dissolved in 10 mL of polyphosphoric acid. The stirred mixture was maintained at 190 °C for 16 h. Thereafter, the solution was allowed to reach room temperature (around 25 °C) and slowly stirred in approximately 20 mL of ice. The reaction mixture was neutralized with NaOH. After the mixture was allowed to stand at room temperature for 1 h, the precipitate was filtered out and washed with water. The solid was recrystallized from ethanol, yielding a white solid for [2] and a red solid for [3]. The protonated salt was synthesized by suspending solid [2] or [3] in acetonitrile and adding 4 equiv of trifluoromethanesulfonic acid (350 μL) to render the corresponding tetraacid triflate salt [2·H₄][CF₃SO₃]₄ or [3·H₄][CF₃SO₃]₄ in quantitative yield.

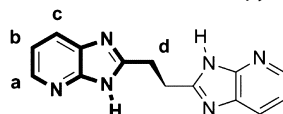
Compound [2]: 1,2-Bis(3H-imidazo[4,5-c]pyridin-2-yl)ethane.



White solid (0.270 g, yield 51%, mp 345 °C). ^1H NMR (DMSO-*d*₆, 270 MHz): δ 8.77 (d, $^4J_{a-b} = 1.0$ Hz, 2H, H_a), 8.19 (d, $^3J_{c-b} = 5.4$ Hz, 2H, H_c), 7.46 (dd, $^4J_{b-a} = 1.0$ Hz, $^3J_{b-c} = 5.4$ Hz, 2H, H_b), 3.42 (s, 4H, H_d). ^{13}C NMR (DMSO-*d*₆, 68 MHz): δ 141.0 (C_c), 138.8 (C_a), 109.4 (C_b), 27.2 (C_d). HRMS-ESI (*m/z*): calcd for [2 + H]⁺ C₁₄H₁₃N₆, 265.1196; found, 265.1199 (error: 1.4 ppm).

Data for [2·H₄][CF₃SO₃]₄: ^1H NMR (DMSO-*d*₆, 300 MHz): δ 8.80 (d, $^4J_{a-b} = 0.6$ Hz, 2H, H_a), 8.23 (d, $^3J_{c-b} = 5.5$ Hz, 2H, H_c), 7.48 (dd, $^4J_{b-a} = 0.6$ Hz, $^3J_{b-c} = 5.5$ Hz, 2H, H_b), 3.46 (s, 4H, H_d). ^1H NMR (CD₃CN, 300 MHz): δ 9.37 (s, 2H, H_a), 8.67 (d, $^3J_{c-b} = 6.7$ Hz, 2H, H_c), 8.32 (d, $^3J_{b-c} = 6.7$ Hz, 2H, H_b), 3.90 (s, 4H, H_d).

Compound [3]: 1,2-Bis(3H-imidazo[4,5-b]pyridin-2-yl)ethane.

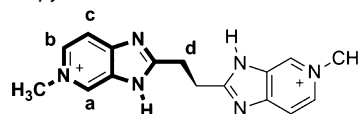


Red solid (0.280 g, yield 53%, mp 360 °C). ^1H NMR (DMSO-*d*₆, 400 MHz): δ 8.23 (d, $^3J_{a-b} = 4.5$ Hz, 2H, H_a), 7.85 (d, $^3J_{c-b} = 7.6$ Hz, 2H, H_c), 7.14 (dd, $^3J_{b-a} = 4.5$ Hz, $^3J_{b-c} = 7.6$ Hz, 2H, H_b), 3.43 (s, 4H, H_d). ^{13}C NMR (DMSO-*d*₆, 68 MHz): δ 143.3 (C_a), 123.0 (C_c), 117.8 (C_b), 27.0 (C_d). HRMS-ESI (*m/z*): [3 + H]⁺ calcd for C₁₄H₁₃N₆, 265.1196; found, 265.1204 (error: 2.9 ppm).

Data for [3·H₄][CF₃SO₃]₄: ^1H NMR (DMSO-*d*₆, 400 MHz): δ 8.48 (d, $^3J_{a-b} = 5.0$ Hz, 2H, H_a), 8.23 (d, $^3J_{c-b} = 8.0$ Hz, 2H, H_c), 7.46 (dd, $^3J_{b-c} = 8.0$ Hz, $^3J_{b-a} = 5.0$ Hz, 2H, H_b), 3.63 (s, 4H, H_d). ^1H NMR (CD₃CN, 300 MHz): δ 8.65 (d, $^3J_{c-b} = 8.2$ Hz, 2H, H_c), 8.59 (d, $^3J_{a-b} = 5.5$ Hz, 2H, H_a), 7.81 (dd, $^3J_{b-c} = 8.2$ Hz, $^3J_{b-a} = 5.5$ Hz, 2H, H_b), 3.80 (s, 4H, H_d).

General Synthesis of Alkyl Derivatives [2·R₂][CF₃SO₃]₂ and [3·R₂][CF₃SO₃]₂. A mixture of compound [2] or [3] (0.25 g, 0.95 mmol) and the corresponding alkyl halide (4.7 mmol) (iodomethane, benzyl bromide, or 4-*tert*-butylbenzyl bromide) was heated under reflux in acetonitrile for 5–7 days. After the mixture was cooled to room temperature (around 25 °C), the precipitate was separated by filtration, washed with chloroform (5 mL \times 3) and air-dried. The obtained solid was dissolved in the minimum amount of hot water, and 4 equiv of sodium trifluoromethanesulfonate (1.3 g, 7.6 mmol) was added. The solution was heated for 1 h and allowed to cool to room temperature (around 25 °C). The precipitate was filtered off, washed with cold water, and air-dried to render the corresponding triflate salt [2·R₂][CF₃SO₃]₂ or [3·R₂][CF₃SO₃]₂ in quantitative yield.

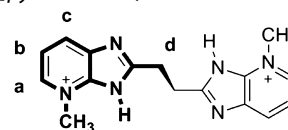
Compound [2·Me₂][CF₃SO₃]₂: 2,2'-(Ethane-1,2-diyl)bis(4-methyl-3H-imidazo[4,5-c]pyridin-4-ium) Trifluoromethanesulfonate.



White solid (0.370 g, yield 67%, mp 327 °C). ^1H NMR (CD₃CN, 270 MHz): δ 9.23 (s, 2H, H_a), 8.47 (d, $^3J_{b-c} = 6.8$ Hz, 2H, H_b), 8.16 (d, $^3J_{c-b} = 6.8$ Hz, 2H, H_c), 4.39 (s, 6H, CH₃), 3.80 (s, 4H, H_d). ^{13}C NMR (CD₃CN, 68 MHz): δ 139.5 (C_c), 136.2 (C_a), 112.1 (C_b), 48.4 (CH₃), 24.9 (C_d). HRMS-ESI (*m/z*): calcd for [2·Me₂]²⁺ C₁₆H₁₈N₆, 147.0791; found, 147.0795 (error: 2.7 ppm).

Data for [2·Me₂H₂][CF₃SO₃]₄: ^1H NMR (CD₃CN, 300 MHz): δ 9.31 (s, 2H, H_a), 8.53 (d, $^3J_{b-c} = 6.4$ Hz, 2H, H_b), 8.25 (d, $^3J_{c-b} = 6.4$ Hz, 2H, H_c), 4.43 (s, 6H, CH₃), 3.86 (s, 4H, H_d).

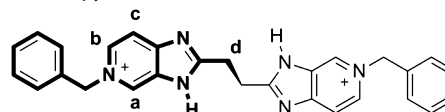
Compound [3·Me₂][CF₃SO₃]₂: 2,2'-(Ethane-1,2-diyl)bis(4-methyl-3H-imidazo[4,5-b]pyridin-4-ium) Trifluoromethanesulfonate.



Red solid (0.410 g, yield 73%, mp 273 °C). ^1H NMR (CD₃CN, 400 MHz): δ 8.53 (d, $^3J_{a-b} = 8.1$ Hz, 2H, H_a), 8.39 (d, $^3J_{c-b} = 6.2$ Hz, 2H, H_c), 7.63 (dd, $^3J_{b-c} = 6.2$ Hz, $^3J_{b-a} = 8.1$ Hz, 2H, H_b), 4.32 (s, 6H, CH₃), 3.73 (s, 4H, H_d). ^{13}C NMR (CD₃CN, 100 MHz): δ 138.2 (C_c), 128.1 (C_a), 118.6 (C_b), 41.3 (CH₃), 26.6 (C_d). HRMS-ESI (*m/z*): calcd for [3·Me₂ + CF₃SO₃]⁺ C₁₇H₁₈F₃N₆O₃S, 443.1108; found, 443.1106 (error: 0.5 ppm).

Data for [3·Me₂H₂][CF₃SO₃]₄: ^1H NMR (CD₃CN, 300 MHz): δ 8.54 (d, $^3J_{a-b} = 8.1$ Hz, 2H, H_a), 8.42 (d, $^3J_{c-b} = 6.2$ Hz, 2H, H_c), 7.66 (dd, $^3J_{b-c} = 6.4$ Hz, $^3J_{b-a} = 8.0$ Hz, 2H, H_b), 4.35 (s, 6H, CH₃), 3.75 (s, 4H, H_d).

Compound [2·Bn₂][CF₃SO₃]₂: 2,2'-(Ethane-1,2-diyl)bis(4-benzyl-3H-imidazo[4,5-c]pyridin-4-ium) Trifluoromethanesulfonate.

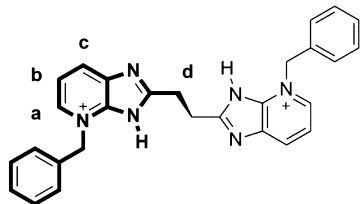


White solid (0.420 g, yield 69%, mp 278 °C). ^1H NMR (CD₃CN, 400 MHz): δ 9.11 (d, $^4J_{a-b} = 1.0$ Hz, 2H, H_a), 8.40 (dd, $^3J_{b-c} = 6.8$ Hz, $^4J_{b-a} = 1.0$ Hz, 2H, H_b), 7.99 (d, $^3J_{c-b} = 6.8$ Hz, 2H, H_c), 7.43 (m, 10H, H_{Ar}), 5.72 (s, 4H, CH₂Ar), 3.63 (s, 4H, H_d). ^{13}C NMR (CD₃CN, 68 MHz): δ 142.4 (C_c), 140.7 (C_{ipso}), 136.3 (C_a),

132.6 (C_{ipso}), 130.4–130.6 (C_{Ar}), 122.6 (C_{ipso}), 115.1 (C_{b}), 66.4 ($C_{\text{CH}_2\text{Ar}}$), 25.2 (C_{d}). HRMS-ESI (m/z): calcd for $[2\text{-Bn}_2 + \text{CF}_3\text{SO}_3]^+ \text{C}_{29}\text{H}_{26}\text{F}_3\text{N}_6\text{O}_3\text{S}$, 595.1734; found, 595.1724 (error: 1.6 ppm).

Data for $[2\text{-Bn}_2\text{H}_2][\text{CF}_3\text{SO}_3]_4$: ^1H NMR (CD_3CN , 300 MHz): δ 9.39 (s, 2H, H_{a}), 8.60 (d, $^3J_{\text{b-c}} = 6.9$ Hz, 2H, H_{b}), 8.20 (d, $^3J_{\text{c-b}} = 6.9$ Hz, 2H, H_{c}), 7.47 (m, 10H, H_{Ar}), 5.80 (s, 4H, CH_2Ar), 3.89 (s, 4H, H_{d}).

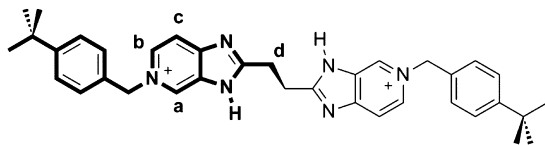
Compound $[3\text{-Bn}_2][\text{CF}_3\text{SO}_3]_2$: 2,2'-(Ethane-1,2-diyl)bis(4-benzyl-3H-imidazo[4,5-b]pyridin-4-ium) Trifluoromethanesulfonate.



Brown solid (0.410 g, yield 68%). ^1H NMR (CD_3CN , 270 MHz): δ 8.48 (m, 4H, $H_{\text{a}} + H_{\text{c}}$), 7.63 (dd, $^3J_{\text{b-c}} = 6.4$ Hz, $^3J_{\text{b-a}} = 8.0$ Hz, 2H, H_{b}), 7.16 (m, 10H, H_{Ar}), 5.79 (s, 4H, CH_2Ar), 3.76 (s, 4H, H_{d}). ^{13}C NMR (CD_3CN , 68 MHz): δ 148.6 (C_{ipso}), 136.7 (C_{c}), 133.7 (C_{ipso}), 131.8 (C_{a}), 128–130 (C_{Ar}), 119.1 (C_{b}), 57.3 ($C_{\text{CH}_2\text{Ar}}$), 25.9 (C_{d}). HRMS-ESI (m/z): calcd for $[3\text{-Bn}_2 + \text{CF}_3\text{SO}_3]^+ \text{C}_{29}\text{H}_{26}\text{F}_3\text{N}_6\text{O}_3\text{S}$, 595.1734; found, 595.1734 (error: 0.1 ppm).

Data for $[3\text{-Bn}_2\text{H}_2][\text{CF}_3\text{SO}_3]_4$: ^1H NMR (CD_3CN , 270 MHz): δ 8.47 (m, 4H, $H_{\text{a}} + H_{\text{c}}$), 7.65 (dd, $^3J_{\text{b-c}} = 6.3$ Hz, $^3J_{\text{b-a}} = 8.2$ Hz, 2H, H_{b}), 7.18 (m, 10H, H_{Ar}), 5.79 (s, 4H, CH_2Ar), 3.77 (s, 4H, H_{d}).

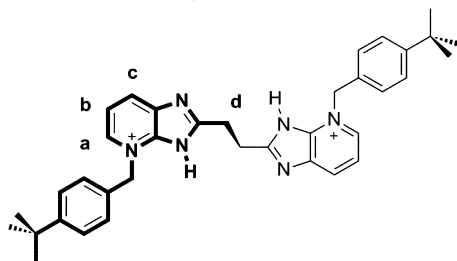
Compound $[2\text{-(tBuBn)}_2][\text{CF}_3\text{SO}_3]_2$: 2,2'-(Ethane-1,2-diyl)bis(4-(4-tert-butylbenzyl)-3H-imidazo[4,5-c]pyridin-4-ium) Trifluoromethanesulfonate.



White solid (0.236 g, yield 29%, mp >360 °C). ^1H NMR (CD_3CN , 400 MHz): δ 9.13 (d, $^4J_{\text{a-b}} = 0.8$ Hz, 2H, H_{a}), 8.41 (dd, $^3J_{\text{b-c}} = 6.8$ Hz, $^4J_{\text{b-a}} = 1.5$ Hz, 2H, H_{b}), 8.00 (d, $^3J_{\text{c-b}} = 6.8$ Hz, 2H, H_{c}), 7.47 (d, $^3J_{\text{H-H}} = 8.5$ Hz, 4H, H_{Ar}), 7.36 (d, $^3J_{\text{H-H}} = 8.5$ Hz, 4H, H_{Ar}), 5.68 (s, 4H, $H_{\text{CH}_2\text{Ar}}$), 3.63 (s, 4H, H_{d}), 1.27 (s, 18H, H_{tBu}). ^{13}C NMR (CD_3CN , 100 MHz): δ 152.9 (C_{ipso}), 137.4 (C_{b}), 136.8 (C_{a}), 134.9 (C_{ipso}), 131.4 (C_{ipso}), 129.4–127.3 (C_{Ar}), 111.6 (C_{c}), 63.5 ($C_{\text{CH}_2\text{Ar}}$), 34.4 ($C_{\text{ipso}}\text{tBu}$), 30.4 (C_{tBu}), 26.0 (C_{d}). HRMS-ESI (m/z): calcd for $[2\text{-(tBuBn)}_2 + \text{CF}_3\text{SO}_3]^+ \text{C}_{37}\text{H}_{42}\text{F}_3\text{N}_6\text{O}_3\text{S}$, 707.2986; found, 707.2989 (error: 0.4 ppm).

Data for $[2\text{-(tBuBn)}_2\text{H}_2][\text{CF}_3\text{SO}_3]_4$: ^1H NMR (CD_3CN , 400 MHz): δ 9.43 (d, $^4J_{\text{a-b}} = 0.5$ Hz, 2H, H_{a}), 8.61 (dd, $^3J_{\text{b-c}} = 6.9$ Hz, $^4J_{\text{b-a}} = 1.3$ Hz, 2H, H_{b}), 8.20 (d, $^3J_{\text{c-b}} = 6.3$ Hz, 2H, H_{c}), 7.49 (d, $^3J_{\text{H-H}} = 8.7$ Hz, 4H, H_{Ar}), 7.41 (d, $^3J_{\text{H-H}} = 8.4$ Hz, 4H, H_{Ar}), 5.77 (s, 4H, $H_{\text{CH}_2\text{Ar}}$), 3.81 (s, 4H, H_{d}), 1.29 (s, 18H, H_{tBu}).

Compound $[3\text{-(tBuBn)}_2][\text{CF}_3\text{SO}_3]_2$: 2,2'-(Ethane-1,2-diyl)bis(4-(4-tert-butylbenzyl)-3H-imidazo[4,5-b]pyridin-4-ium) Trifluoromethanesulfonate.



Red solid (0.236 g, yield 29%, mp 180 °C). ^1H NMR (CD_3CN , 400 MHz): δ 8.49 (m, 4H, $H_{\text{a}} + H_{\text{c}}$), 7.64 (dd, $^3J_{\text{b-c}} = 6.3$ Hz, $^3J_{\text{b-a}} = 8.0$ Hz, 2H, H_{b}), 7.13 (d, $^3J_{\text{H-H}} = 8.6$ Hz, 4H, H_{Ar}), 7.02

(d, $^3J_{\text{H-H}} = 8.6$ Hz, 4H, H_{Ar}), 5.80 (s, 4H, CH_2Ar), 3.83 (s, 4H, H_{d}), 1.13 (s, 18H, H_{tBu}). ^{13}C NMR (CD_3CN , 100 MHz): δ 137.5 (C_{c}), 129.3 (C_{a}), 126.8–129.5 (C_{Ar}), 120.2 (C_{b}), 57.9 ($C_{\text{CH}_2\text{Ar}}$), 31.4 (C_{tBu}), 26.8 (C_{d}). HRMS-ESI (m/z): calcd for $[3\text{-(tBuBn)}_2]^{2+} \text{C}_{36}\text{H}_{42}\text{N}_6$, 279.1730; found, 279.1733 (error: 1.0 ppm).

Data for $[3\text{-(tBuBn)}_2\text{H}_2][\text{CF}_3\text{SO}_3]_4$: ^1H NMR (CD_3CN , 270 MHz): δ 9.03 (d, $^3J_{\text{a-b}} = 7.8$ Hz, 2H, H_{a}), 8.74 (d, $^3J_{\text{c-b}} = 5.8$ Hz, 2H, H_{c}), 8.16 (dd, $^3J_{\text{b-c}} = 6.3$ Hz, $^3J_{\text{b-a}} = 8.5$ Hz, 2H, H_{b}), 7.59 (d, $^3J_{\text{H-H}} = 8.5$ Hz, 4H, H_{Ar}), 7.46 (d, $^3J_{\text{H-H}} = 8.5$ Hz, 4H, H_{Ar}), 6.00 (s, 4H, CH_2Ar), 4.12 (s, 4H, H_{d}), 1.33 (s, 18H, H_{tBu}).

Synthesis of [2]Pseudorotaxane $\{[2\text{-Bn}_2\text{H}_2]\text{CDB24C8}\}[\text{CF}_3\text{SO}_3]_4$. Consecutive additions of 2 equiv of trifluoromethanesulfonic acid (2 μL) and 1 equiv of DB24C8 (50 μL of a 5×10^{-2} M solution) to 0.5 mL of a 5×10^{-3} M solution of compound $[2\text{-Bn}_2][\text{CF}_3\text{SO}_3]_2$ in CD_3CN resulted in the formation of this [2]pseudorotaxane in a slow association/dissociation process on the NMR time scale.

Data for $\{[2\text{-Bn}_2\text{H}_2]\text{CDB24C8}\}[\text{CF}_3\text{SO}_3]_4$: ^1H NMR (CD_3CN , 300 MHz): δ 9.13 (s, 2H, H_{a}), 8.53 (d, $^3J_{\text{b-c}} = 6.8$ Hz, 2H, H_{b}), 7.98 (d, $^3J_{\text{c-b}} = 6.8$ Hz, 2H, H_{c}), 7.51 (s, 10H, H_{Ar}), 6.52 (m, 8H, DB), 5.69 (s, 4H, CH_2Ar), 4.09 (s, 4H, H_{d}), 3.89–4.01 (m, 24H, O– CH_2CH_2 –O). HRMS-ESI (m/z): calcd for $[2\text{-Bn}_2\text{CDB24C8} + \text{CF}_3\text{SO}_3]^+ \text{C}_{53}\text{H}_{58}\text{F}_3\text{N}_6\text{O}_{11}\text{S}$, 1043.3831; found, 1043.3821 (error: 0.95 ppm).

X-ray Crystal Structure Determination. Crystals were grown by slow evaporation of (i) a saturated aqueous solution of axle $[2\text{-Bn}_2][\text{CF}_3\text{SO}_3]_2$, (ii) a solution of axle $[3\text{-Bn}_2]\text{Br}_2$ in $\text{CH}_3\text{CN}/\text{CHCl}_3$, and (iii) a saturated solution containing $[2\text{-Bn}_2\text{H}_2][\text{CF}_3\text{SO}_3]_4$ and 3 equiv of DB24C8 in CH_3CN . Crystals were mounted on a glass fiber. A full hemisphere of data were collected with 30 s frames on a Enraf–Nonius Kappa diffractometer fitted with a CCD-based detector using Mo $K\alpha$ radiation (0.71073 Å). The diffraction data and unit-cell parameters were consistent with the assigned space groups. The structures were solved by direct methods, completed by subsequent Fourier syntheses, and refined with full-matrix least-squares methods against I^2 data. All non-hydrogen atoms were refined anisotropically. All hydrogen atoms were treated as idealized contributions. Scattering factors and anomalous dispersion coefficients are contained in the SHELXTL 5.03 program library.¹⁵ Ball-and-stick and space-filling diagrams were prepared using DIAMOND 3.0.¹⁶

Crystal structure data for $[2\text{-Bn}_2][\text{CF}_3\text{SO}_3]_2 \cdot \text{H}_2\text{O}$: $\text{C}_{30}\text{H}_{30}\text{F}_3\text{N}_6\text{O}_8\text{S}_2$, $M = 780.72$, monoclinic, $a = 11.281(2)$ Å, $b = 8.829(2)$ Å, $c = 17.148(3)$ Å, $\beta = 95.77(3)^\circ$, $V = 1699.4(6)$ Å³, $T = 293(2)$ K, space group $P2_1/c$, $Z = 2$, $D_{\text{calcd}} = 1.526$ g cm⁻³, $\mu(\text{Mo K}\alpha) = 0.249$ mm⁻¹, $R_1 = 0.1207$ for 3622 F_o , $> 4\sigma(F_o)$ and 0.2030 for all data, $wR_2 = 0.2448$, GOF = 1.194.

Crystal structure data for $[3\text{-Bn}_2]\text{Br}_2 \cdot \text{CHCl}_3$: $\text{C}_{29}\text{H}_{27}\text{Cl}_3 \text{Br}_2\text{N}_6$, $M = 725.74$, monoclinic, $a = 9.925(1)$ Å, $b = 12.232(1)$ Å, $c = 25.401(1)$ Å, $\beta = 97.864(1)^\circ$, $V = 30.547(5)$ Å³, $T = 293(2)$ K, space group $P2_1/n$, $Z = 4$, $D_{\text{calcd}} = 1.578$ g cm⁻³, $\mu(\text{Mo K}\alpha) = 2.946$ mm⁻¹, $R_1 = 0.0746$ for 5507 F_o , $> 4\sigma(F_o)$ and 0.1652 for all data, $wR_2 = 0.1652$, GOF = 1.031.

Crystal structure data for $[2\text{-Bn}_2\text{H}_2\text{CDB24C8}][\text{CF}_3\text{SO}_3]_4$: $\text{C}_{56}\text{H}_{60}\text{F}_{12}\text{N}_6\text{O}_{20}\text{S}_4$, $M = 1493.34$, monoclinic, $a = 12.368(3)$ Å, $b = 10.385(3)$ Å, $c = 25.353(5)$ Å, $\beta = 90.87(3)^\circ$, $V = 3256.3(1)$ Å³, $T = 293(2)$ K, space group $P2_1/n$, $Z = 2$, $D_{\text{calcd}} = 1.523$ g cm⁻³, $\mu(\text{Mo K}\alpha) = 0.258$ mm⁻¹, $R_1 = 0.0939$ for 5705 F_o , $> 4\sigma(F_o)$ and 0.1949 for all data, $wR_2 = 0.1949$, GOF = 1.058.

CCDC-953101 for $[2\text{-Bn}_2][\text{CF}_3\text{SO}_3]_2 \cdot \text{H}_2\text{O}$, CCDC-953103 for $[3\text{-Bn}_2]\text{Br}_2 \cdot \text{CHCl}_3$, and CCDC-953102 for $[2\text{-Bn}_2\text{H}_2\text{CDB24C8}][\text{CF}_3\text{SO}_3]_4$ contain the supplementary crystallographic data for this paper. These data can be obtained free of charge from The Cambridge Crystallographic Data Center via http://www.ccdc.cam.ac.uk/data_request/cif.

General Procedures for the K_a Measurements. Single-Point Method. An ^1H NMR spectrum of an equimolar solution (5.0×10^{-3} M) of cation $[2\text{-Bn}_2\text{H}_2][\text{CF}_3\text{SO}_3]_4$ and dibenzo-24-crown-8 ether in CD_3CN was recorded at 25 °C. The concentrations of all the species at equilibrium were determined using the initial concentrations and the integration of the aromatic resonances of uncomplexed and complexed species.

Least-Squares Fitting Analysis. The association constants were determined from a ^1H NMR titration at 25 °C in CD_3CN by a

least-squares fitting analysis of the chemical shifts of proton H_b using the software WinEQNMR2¹⁷ at a concentration of 2×10^{-3} M.

■ ASSOCIATED CONTENT

■ Supporting Information

Copies of ¹H and ¹³C NMR spectra for the reported compounds as well as crystallographic data (CIF). This material is available free of charge via the Internet at <http://pubs.acs.org>.

■ AUTHOR INFORMATION

Corresponding Author

*Tel: (+52) 55 57 47 37 21. Fax: (+52) 55 57 47 33 89. E-mail: jtiburcio@cinvestav.mx.

Notes

The authors declare no competing financial interest.

■ ACKNOWLEDGMENTS

This work was financially supported by Conacyt - México (Project 128419). We thank Marco Leyva and Geiser Cuellar for their assistance with obtaining X-ray data and mass spectra, respectively, and Raúl I. Sánchez-Alarcón for his support in the titration experiments.

■ REFERENCES

- (1) (a) *Catenanes, Rotaxanes and Knots*; Sauvage, J.-P., Dietrich-Buchecker, C., Eds.; Wiley-VCH: Weinheim, Germany, 1999. (b) Kay, E. R.; Leigh, D. A.; Zerbetto, F. *Angew. Chem., Int. Ed.* **2007**, *46*, 72. (c) Balzani, V.; Venturi, M.; Credi, A. *Molecular Devices and Machines: Concepts and Perspectives for the Nano World*; Wiley-VCH: Weinheim, Germany, 2008.
- (2) (a) Rowan, S. J.; Cantrill, S. J.; Cousins, G. R. L.; Sanders, J. K. M.; Stoddart, J. F. *Angew. Chem., Int. Ed.* **2002**, *41*, 898. (b) Meyer, C. D.; Joiner, C. S.; Stoddart, J. F. *Chem. Soc. Rev.* **2007**, *36*, 1705. (c) Hubin, T. J.; Busch, D. H. *Coord. Chem. Rev.* **2000**, *200–202*, 5. (d) Aricó, F.; Badjic, J. D.; Cantrill, S. J.; Flood, A. H.; Leung, K. C.-F.; Stoddart, J. F. *Top. Curr. Chem.* **2005**, *249*, 203.
- (3) (a) Spence, G. T.; Beer, P. D. *Acc. Chem. Res.* **2013**, *46*, 571. (b) Serpell, C. J.; Kilah, N. L.; Costa, P. J.; Félix, V.; Beer, P. D. *Angew. Chem., Int. Ed.* **2010**, *49*, 5322.
- (4) Noujeim, N.; Leclercq, L.; Schmitzer, A. R. *J. Org. Chem.* **2008**, *73*, 3784.
- (5) (a) Wang, R.; Yuan, L.; Macartney, D. H. *Chem. Commun.* **2006**, 2908. (b) Kolman, V.; Marek, R.; Strelcova, Z.; Kulhanek, P.; Necas, M.; Svec, J.; Sindelar, V. *Chem.—Eur. J.* **2009**, *15*, 6926. (c) Biedermann, F.; Rauwald, U.; Cziferszky, M.; Williams, K. A.; Gann, L. D.; Guo, B. Y.; Urbach, A. R.; Bielawski, C. W.; Scherman, O. A. *Chem.—Eur. J.* **2010**, *16*, 13716.
- (6) Ling, I.; Alias, Y.; Sobolev, A. N.; Byrne, L. T.; Raston, C. L. *Chem.—Eur. J.* **2010**, *16*, 6973.
- (7) (a) Li, C.; Zhao, L.; Li, J.; Ding, X.; Chen, S.; Zhang, Q.; Yu, Y.; Jia, X. *Chem. Commun.* **2010**, *46*, 9016. (b) Li, C.; Shu, X.; Li, J.; Chen, S.; Han, K.; Xu, M.; Hu, B.; Yu, Y.; Jia, X. *J. Org. Chem.* **2011**, *76*, 8458.
- (8) Reyes-Márquez, V.; Tiburcio, J.; Höpfl, H.; Sanchez-Vazquez, M.; Hernández-Ahuactzid, I. F.; Moreno-Corral, R.; Lara, K. O. *J. Phys. Org. Chem.* **2012**, *25*, 1042.
- (9) (a) Castillo, D.; Astudillo, P.; Mares, J.; González, F. J.; Vela, A.; Tiburcio, J. *Org. Biomol. Chem.* **2007**, *5*, 2252. (b) Li, L.; Clarkson, G. *J. Org. Lett.* **2007**, *9*, 497.
- (10) (a) Zhu, K.; Vukotic, N.; Loeb, S. J. *Angew. Chem., Int. Ed.* **2012**, *51*, 2168. (b) Noujeim, N.; Zhu, K.; Vukotic, N.; Loeb, S. J. *Org. Lett.* **2012**, *14*, 2484. (c) Zhu, K.; Vukotic, N.; Noujeim, N.; Loeb, S. J. *Chem. Sci.* **2012**, *3*, 3265.
- (11) (a) Ashton, P. R.; Chrystal, E. J. T.; Glink, P. T.; Menzer, S.; Schiavo, C.; Spencer, N.; Stoddart, J. F.; Tasker, P. A.; White, A. J. P.;

Williams, D. J. *Chem.—Eur. J.* **1996**, *2*, 709. (b) Loeb, S. J.; Tiburcio, J.; Vella, S. J.; Wisner, J. A. *Org. Biomol. Chem.* **2006**, *4*, 667.

(12) (a) Ashton, P. R.; Baxter, I.; Fyfe, M. C. T.; Raymo, F. M.; Spencer, N.; Stoddart, J. F.; White, A. J. P.; Williams, D. J. *J. Am. Chem. Soc.* **1998**, *120*, 2297. (b) Loeb, S. J.; Wisner, J. A. *Angew. Chem., Int. Ed.* **1998**, *37*, 2838. (c) Mercer, D. J.; Vella, S. J.; Guertin, L.; Suhan, N. D.; Tiburcio, J.; Vukotic, V. N.; Wisner, J. A.; Loeb, S. J. *J. Org. Chem.* **2011**, 1763.

(13) The observed chemical shifts may reflect an average of different supramolecular co-conformations.

(14) (a) Huang, F.; Jones, J. W.; Slobodnick, C.; Gibson, H. W. *J. Am. Chem. Soc.* **2003**, *125*, 14458. (b) Li, J.-S.; Chen, L.-G.; Zhang, Y.-Y.; Xu, Y.-J.; Deng, Y.; Zeng, T.; Huang, P.-M. *J. Chem. Res.* **2007**, 350. (c) Cervantes, R.; Sánchez, R. I.; Tiburcio, J. *Chem.—Eur. J.* **2013**, *19*, 4051.

(15) Sheldrick, G. M. *SHELXTL 6.14 Program Library*; Brüker Analytical Instrument Division: Madison, WI, 2003.

(16) *DIAMOND 3.0: Visual Crystal Structure Information System*; Crystal Impact: Bonn, Germany, 2004.

(17) Hynes, M. J. *J. Chem. Soc., Dalton Trans.* **1993**, 311.